IOP Conf. Series: Materials Science and Engineering **118** (2016) 012019 doi:10.1088/1757-899X/118/1/012019

Experimental and numerical investigation on cold flat rolling processes of DC04 sheets with special focus on residual stresses

A Bauer[1,2], T Mehner[3], C Binotsch[2], M Sieber[3], B Awiszus[2] and T Lampke[3]

[1] Corresponding author, email: a.bauer@mb.tu-chemnitz.de
[2] Chair of Virtual Production Engineering, Institute for Machine Tools and Production Processes, Technische Universität Chemnitz, 09125 Chemnitz, Germany
[3] Materials and Surface Engineering Group, Institute of Materials Science and Engineering, Technische Universität Chemnitz, 09125 Chemnitz, Germany

Abstract. The process of cold flat rolling is a widespread industrial technique to manufacture semi-finished products, e.g., for the automotive or homewares industry. Basic knowledge of the process regarding dimensioning and adjustment of defined characteristics is already state of the art. However, a detailed consideration and analysis with respect to local inhomogeneous residual stresses in several process steps mostly remains disregarded. A broad understanding of the process due to the distribution of residual stresses in the workpiece and the direction of the stress tensors allows for a definition of the characteristics of the workpiece even before the actual manufacturing process. For that purpose, it is necessary to perform numerical investigations by means of the finite element analysis (FEA) of cold flat rolling processes.
Within this contribution, several approaches for the calibration of the FEA with the real flat rolling process will be addressed and discussed. To ensure that the numerical consideration provides realistic results, this calibration is indispensable. General parameters such as geometry, height reduction, rolling temperature, process time, and the rolling speed are considered as well as a photogrammetric survey, and calculated residual stresses with results of X-ray diffraction (XRD) will be compared.
In the course of the experiments, a good agreement between the stress results of the FEA and the XRD was found in the center of the specimen. In combination with the allocation of the stress orientations, the agreement close to the edges is also fine. Some issues that cause differences between the FEA and the experiment are dis-cussed.

1. Introduction

The process of cold flat rolling is a widespread industrial technique to manufacture semi-finished products, e.g., for the automotive or homewares industry. The normal procedure for the cold strip production is divided in the following six main components: pickling, cold rolling, annealing, skin pass rolling, refinement and adjustment. One of the major tasks of cold flat rolling is the defined adjustment of measurements, material homogeneity, surface quality like roughness or waviness, and the mechanical properties [1]. The quality of the hot rolling strip has a big influence on the achievable results in the cold rolling process because cold rolling is mostly situated at the end of the process chain. With a good understanding of the process parameters, it is possible to influence the mechanical properties in a defined way, even at this time of the process. Ideally, a defined rolling state without any following post treatment (e.g., heat) can be achieved. Therefore, it is necessary to acquire a good knowledge of the effects of different parameters on the cold rolling process. A good way of taking most of those parameters into account is a well calibrated finite elements analysis (FEA). With the help of the FEA, it is possible to analyze the process numerically under variation of different parameters. Some of the most important results related to the mechanical properties are residual stresses. These residual stresses are a major part of this consideration. A deeper understanding of the evolution, direction and expression of these stresses mostly remains unconsidered. Just a few authors analyzed residual stresses in forming processes in a more detailed way [e.g., 2, 3, 4, 5, 6], but even they do not analyze the orientation of the stress tensors and the basic cold flat rolling processes.

2. Experimental and simulative setup

The material used for the experiments is a general DC04 sheet metal (*Max Baum Stahl Service GmbH*). It is very important to choose an ordinary steel with a small proportion of alloying elements to gain understanding of the basic processes without phase transformations or further micromechanical problems. The material composition is given with 0.042 % C, 0.242 % Mn, 0.010 % P, 0.013 % S, 0.035 % Al, 0.011 % Si, and Fe balance [7]. The roughness average of the used DC04 is about $R_a = 0.99 \pm 0.09$ µm in rolling direction. Prior to rolling, the metal sheets were cut into samples with the dimensions of 100 mm × 14 mm × 2 mm by water jet cutting. Water jet cutting was used to avoid additional shear or tensile stresses induced by the cutting process.

After cutting, the samples were rolled at room temperature on a *Duo/Quarto EW 105x100* strip rolling mill by *Bühler & Co GmbH*. This rolling mill is especially designed for experimental purposes. The roll speed can be varied from 3.0 rpm to 24.3 rpm with a roll diameter of 105 mm. The defined consistent roll speed in the experiments was selected to be 12.12 rpm. The constant rolling force within the rolling mill is specified with a maximum of 100 kN while using the duo mode with 2 working rolls. The samples were loaded manually until they overcame the roll feed and proceeded through the rotary movement of the working rolls. The distance of the rolls can be adjusted with a step size of 10 µm.

While processing the samples, a thickness reduction of 0.5 mm occurs. Thus, the thickness of the analyzed specimen is 1.5 mm. The evenness of the samples was ensured because bends across the length of the specimen cause a distinct variation of the measured stresses and may even alter the sign of the residual stresses.

The numerical analysis of the flat rolling process was set up in the finite element simulation program *simufact.forming (SF) 13.0*, which is especially appropriate for forming processes. More precisely, the *general purpose (GP) tool* was used, which includes additional functions of importance for rolling processes. With the *simufact.forming general purpose tool* (SF GP), it is possible to generate a defined mesh over for the specimen, which can be manually positioned.

Remeshing of the sample is possible but was not applied. Related special characteristics concerning the process are discussed in detail in chapter 4. In general, the numerical model was generated with 8-node-hexahedral elements with the size of 0.500 mm × 0.250 mm × 0.125 mm. Furthermore, the simulative model was set up as 3D mechanical simulation. In the numerical analysis with SF GP, thermal effects were generally not taken into account because only minor temperature increases of about 15–20 °C occurred. But for calibrating the results, a coupled analysis of mechanical and thermal effects was performed once. The material model for the used DC04 was defined with a flow curve received from and adjusted by the *Autoform (Autoform Engineering GmbH)* material library. The tools were defined as rigid bodies and the kinematics were transferred from the real flat rolling process. Between the working rolls and the sample, a combined friction coefficient of $\mu = 0.35$ was added. Furthermore, an additional pusher was needed to simulate the mechanical force, which is required to overcome the roll feed. So called "fences" were used to prevent the specimen from bending (figure 1).

During the numerical analysis, the cold flat rolling process is very susceptible to bending due to the contact values and therefore, it is necessary to integrate those fences with $\mu = 0$. As solver, the iterative sparse calculation was used. Within a second process step, the working rolls release the sample to achieve results with no remaining loads on the surface.

Photogrammetric analyzes were performed with *ARGUS* (*Gesellschaft für optische Messtechnik mbH*), which is capable of detecting the shape of an object with only a couple of photos taken from different positions. Therefore, a pattern of circles with a defined diameter of 0.5 mm and a distance of 1 mm was printed electrolytically on the surface of the specimen. Subsequently, the samples were processed in the rolling mill. The pattern elongates during the rolling process. To evaluate the results, the rolled sample was photographed with the ARGUS camera and the deformation of the sample was detected through the deformation of the defined circles. The evaluation was performed with the *ARGUS-Forming-Ananlysis-GOM*-v6.2.0 software. Results are, e.g., the major strain, the minor strain, the *von-Mises* strain, and the reduction of the thickness. The results can be illustrated with a color scale and the

associated distribution over the specimen. For the rolling processes, the interesting values are the major and minor strain as well as the *von-Mises* strain.

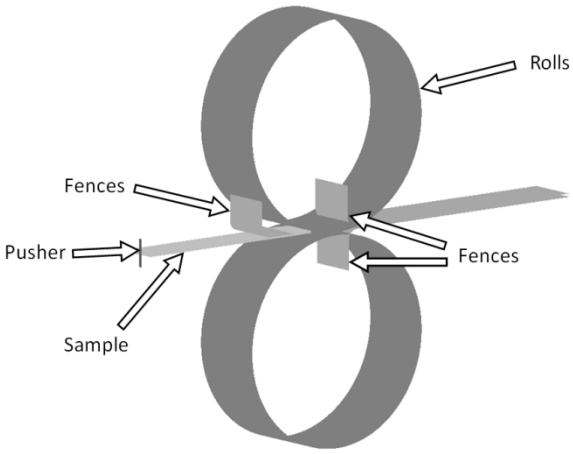

Figure 1. Rolling setup in the simulation model.

Residual stresses were measured using a diffractometer *D8 Discover* (*Bruker AXS*) with cobalt K_α radiation for the X-ray diffraction (XRD) analysis. A pinhole aperture with a diameter of 0.5 mm was used to confine the X-ray beam. Line scans along the y direction were performed starting from the center of the sample measuring 10 positions with a step size of 0.7 mm. The $\sin^2\psi$ method was applied: $\sin^2\psi$ was varied with a step size of 0.1 with both positive and negative ψ values. Three rotation angles around the sample normal were used (φ = 0°, 45°, 90°). The lattice planes {211} of α iron (*Young*'s modulus 220 GPa, *Poisson*'s ratio 0.28 [8]) were measured and evaluated by means of the program *Leptos* (*Bruker AXS*).

3. Calibration of the finite elements model and results

According to the VDI standard 3633, the FEA is a tool, which defines the reproduction of a real process. Due to the fact that the numerical calculation is always just an approximation to the reality, there are also many parameters, which can be adjusted within a numerical model. Those parameters have to be set so that the simulation can generate results, which can be used as a prediction for real processes. To ensure that the numerical model fulfills these criteria, a calibration needs to be performed with the associated process. Without any comparison to the reality, it is very hard to interpret the calculated results in the right way. The significance of simulations without reference to test stands or related processes is not very meaningful. To guarantee that the numerical model shows results similar to the checked problems, there are different options, which are pointed out in the following sections.

3.1. Calibration with standard process parameters

The rolling technology includes some parameters, which are quite easy to prove and calibrate. Among these classic parameters are, for example, geometric measurements. The examined rolling specimen was 100 mm in length (x-axis), 14 mm in width (y-axis) and 2 mm in thickness (z-axis). This geometry was exactly rebuilt in SF GP. During the rolling process, the geometry became elongated, and the y/z ratio of 7 indicated a small widening in the y direction. The sample also expands in the numerical analysis (table 1).

Table 1. Comparison of measurements, temperature and rolling period for the calibration of the simulation with experimental values for the first rolling pass (2.0 mm to 1.5 mm).

Parameter	Experiment	Simulation	Deviation (%)
Sample geometry			
Length (mm)	127.5	128.0	1
Width (mm)	14.5	14.4	< 1
Thickness (mm)	1.50	1.50	< 1
Rolling period (s)	2.3	2.1	9
Temperature (K)	311	310	< 1

Other parameters are the time for one rolling step and the temperature, which was inducted into the specimen (table 1). The time was stopped with a digital chronometer and the temperature was measured with an industrial thermometer on the surface of the specimen directly after each rolling pass. For the calculation of the temperature within the FEA, it is necessary to activate the coupled process for mechanical and thermal effects. This function mostly remains deactivated in the context of cold rolling because it requires additional calculation time. Therefore, it is sufficient to realize this calculation once for every rolling pass if it should be required for the results.

In addition to these standard ways of calibrating numerical simulations, there are some special approaches to achieve well matched processes. These particular tools need a good agreement between reality and simulation. Some methods such as detecting the grain structure for mechanical stress analyses are not appropriate for every kind of numerical analysis. Thus, it must be carefully considered which type of analysis fits the simulation and leads to good parameters for the calibration of the process.

The von-Mises strain measured with the ARGUS GOM system is shown in figure 2. The local influences on the different measuring points within the photogrammetric analysis cause a more irregular distribution of values than in the FEA, but in general, they are at almost the same level. Therefore, it can be inferred that the calibration shows a good agreement. The values of the numerical analysis are at about 0.29–0.30 in the center of the specimen, while the photogrammetric survey lies at about 0.27–0.28.

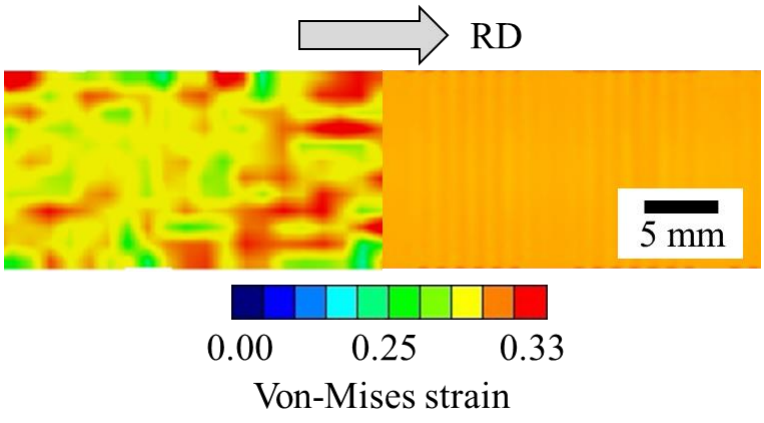

Figure 2. Comparison of von-Mises strain of the GOM-ARGUS (left) and FEA (right) results.

Other important calibration parameters are the residual stresses of the specimen, which are discussed in detail in the following section.

3.2. Calibration of residual stresses

In contrast to hot rolling, during which recovery and recrystallization processes occur and residual stresses are reduced, hardening has to be considered when dealing with cold rolling processes. As a result of the micromechanical properties of cold processed steel, the displacements of the material during the forming process entail that stresses are induced into the specimen. Those stresses lead to a change of the mechanical characteristics of the workpieces. To influence the behavior of the workpiece in a suitable way, it is necessary to understand how and where stresses appear, and how they can be influenced by proper manufacturing. The numerical calculation can be a good tool to prove which factors influence the results in what way. To gain relevant significance, a good calibration between numerical analysis and the real process is needed. The more factors are compared, the better a calibration works. In addition, it is very important to adjust the calibration to the required results. For the consideration in this paper, the analysis of residual stresses constitutes a major part. For this purpose, the XRD method is among other reasons appropriate because of the penetration depth that is comparable with the size of the elements in the FEA. A well calibrated simulation can be used as a tool to predict influences of varying forming parameters.

The residual stresses within the considered specimen evolve in a special way. The flow resistance in y direction is larger compared to the flow resistance in x direction. This circumstance can be ascribed to the geometrical shape in flat rolling because of the distribution of contact surfaces within the rolling gap. Further, there is a bigger amount of contact in width than lengthwise. For that reason, the material principally flows in rolling direction. The bigger the ratio between width (y) and pressed length (in the rolling gap), the lower is the increase in y direction. Another important factor is the relation between width and height of the workpiece. From a y/z ratio > 10, it can be assumed that the rolling process is free of the increase in width [9]. In the case of y/z = 7, the analyzed specimens are situated in the upper areas and are just subject to a minor increase in width of approximately 0.4 mm (rolling step 2.0 mm to 1.5 mm). Through the reduction in thickness, the relation increases to a factor of approximately 9.5 in further rolling passes, which leads to a lower increase in width with every following rolling step.

As a result of the chosen sample geometry, there is a special development of stresses because the material flow in width (y) direction is hindered by the geometry in the rolling gap. Therefore, significantly differing stresses arise at the edges of the sample compared to the center areas. At this point, the knowledge of the general distribution of stresses and of the orientation of the stress tensors is necessary. To achieve an exact calibration of the actual process with the numerical analysis, both the orientation of the residual stresses and their amount has to be analyzed. Through this concept, some conclusions can be drawn in relation to the material flow and the stress development. Hence, an aimed impact on the stresses through the geometry of the rolled material and the rolling tools is possible. In the following, a detailed comparison of the numerical analysis and the XRD will show the accordance and the details of the numerical results.

The typical distribution within the following specimen evolves through the combination of different phenomena. As described above, the material is hindered to flow in y direction due to the geometrical dimensions of sample and rolling gap. Nevertheless, the sample is reduced in thickness as a result of the increasing infeed of the working rolls. Thus, the rolling direction is the only possible direction for the material flow. As a result of the forced material flow in x direction, tensile stresses develop. The tensile stresses are denoted as positive and compressive stresses as negative values. The allocation of stresses takes place in such a way within the SF GP so that the most positive value is called “maximum residual stresses” and the most negative one “minimal residual stresses”. In this way, the maximum residual stresses could be the smallest, according to the amount, if the intermediate and the minimum residual stresses are negative [10]. The intermediate residual stress is typically not taken into consideration because it is often close to zero. Within the XRD, the stresses were given and arranged as follows: The residual stresses are arranged in the order of their amount. In other words, the principal stress with the highest amount is denoted as σ_1, and the one with the lowest amount is called σ_3. According to this principle, the order of stresses between the XRD and the numerical analysis has to be considered additionally. Therefore, the measured values have to be compared and analyzed in advance. To rate the

observed differences between the results of the XRD and the FEA, the measurement uncertainties of both techniques have to be considered. The uncertainties within the XRD account for about ± 10 MPa. For the FEA, uncertainties are more difficult to define due to imperfections of the underlying material model, inaccurate initial material states, and numerical errors that may increase in subsequent simulations. What follows is that only absolute numbers can be estimated. The stress results of the simulation are shown in figure 3, and the comparison with the experimental values can be found in table 2.

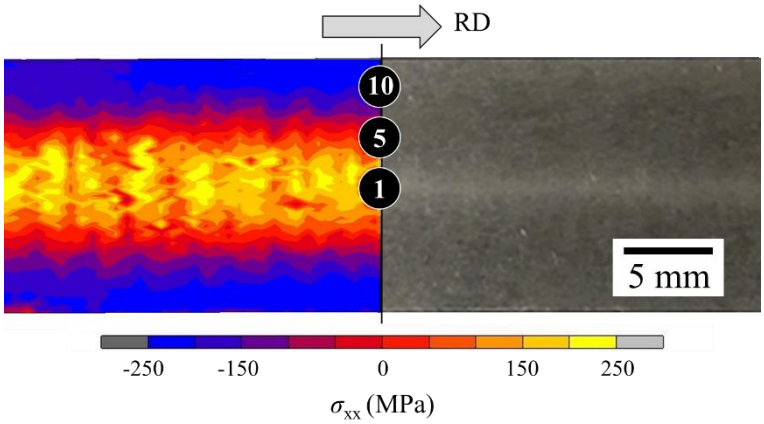

Figure 3. FEA results of σ_{xx} with the marked positions (1–10) for the XRD line scan.

Table 2. Comparison of principal stresses for the calibration of the simulation with experimental values for the rolling pass 2.0 mm to 1.5 mm.

Parameters	Experiment (MPa)	Simulation (MPa)	Difference (MPa)
σ_1 center	240	219	21
σ_1 edges	132	94	38
σ_2 center	18	13	5
σ_2 edges	-73	-100	27

The orientation of the stress tensors can be evaluated in addition to the scalar stress values. Therefore, the described distribution of the stresses can be seen and easily understood. The stress tensors of the maximum principal stresses in the center of the specimen are generally orientated in rolling direction. With increasing distance to the center, the stresses of the specimen are progressively orientated to the edges of the sample and perpendicular to the stresses in the center (figure. 4). This phenomenon occurs because of the above-mentioned experimental procedure in which the material flow in rolling direction (x) is free, while the flow in width direction (y) is hindered. Thus, the described tensile stresses develop. According to the amount, the tensile stresses at the edge of the specimen are clearly lower than the stresses in the center of the sample. Within the minimal principal stress value, the stress behavior is opposite. The simulations reveal that the minimal principal stresses in the center of the sample are almost zero and orientated to the edges of the specimen, the stresses at the edges are large with an almost antiparallel orientation to the rolling direction (RD). Those stresses are orientated in the direction opposite to the rolling direction (figure. 4) because of the prevented material flow in width direction. The corresponding values on the basis of which the development of the tensor direction can be reconstructed are listed in table 3.

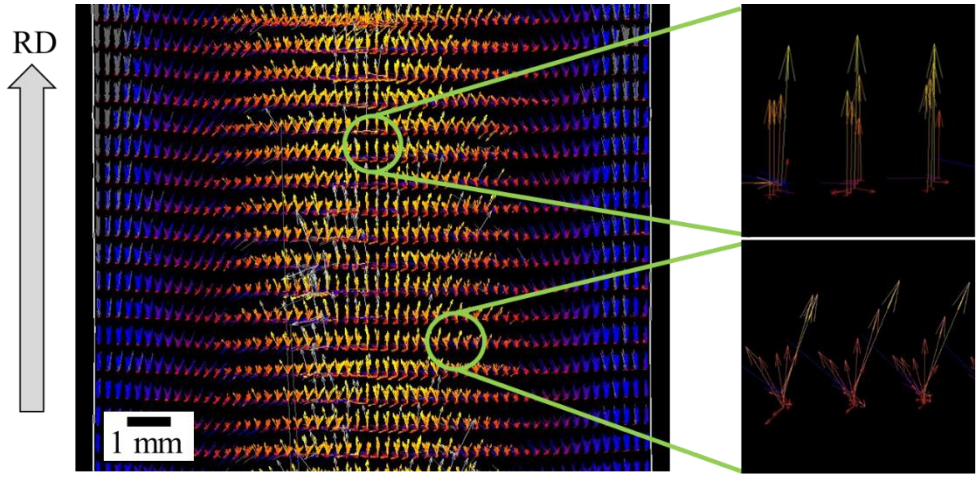

Figure 4. Combined illustration of the orientation of the principal stress tensors of σ_1 and σ_2 (upper inset: orientation in rolling direction; lower inset: increasing deviation of the stress tensors to the rolling direction).

Table 3. Comparison between experimental (exp) and simulative (sim) stresses in (σ_{xx}) and perpendicular (σ_{yy}) to the rolling direction (RD) as well as the orientation of σ_1 and σ_2 for the rolling pass 2.0 mm to 1.5 mm.

Position (figure 3)	Experiment σ_{xx} (MPa)	Simulation σ_{xx} (MPa)	Orientation σ_1 (exp/sim) (° to RD)	Experiment σ_{yy} (MPa)	Simulation σ_{yy} (MPa)	Orientation σ_2 (exp/sim) (° to RD)
1	179	183	-7/ 0.0	-23	-39	82/ 90.0
2	170	172	-2/ 0.0	-70	-35	88/ 90.0
3	179	167	5/ 0.0	-56	-45	96/ 90.0
4	155	116	4/ 0.0	-71	-30	94/ 90.0
5	137	18	4/22.5	-73	-50	94/112.5
6	116	-33	8/22.5	-82	-52	98/112.5
7	98	-122	25/45.0	-70	-51	105/135.0
8	67	-170	29/45.0	-69	-49	109/135.0
9	-40	-184	29/67.5	-126	-43	110/157.5
10	-120	-192	45/67.5	-119	-29	135/157.5

Given the difficulties in quantifying the right angles, the orientation of the stress tensors within the FEA is set up in steps of 22.5°. Within the XRD, the corresponding angles are provided together with the results. Additionally, it should be mentioned at this point that the step size of the positions within the FEA is not the same as used within the XRD. The available distances solely can be changed in steps of 0.25 mm depending on the used distance between the nodes within the FEM (0.7 mm in XRD). Despite of the sometimes differing values at the measuring positions, it can be seen that the stresses within the FEA and the XRD develop in an equivalent way. For example, the stresses with the same orientation in table 3, like σ_{xx} in position 10 (experiment) and position 7 (simulation), both with an angle of 45° to the rolling direction, also correspond with the values of stress: 120 MPa (experiment) and 122 MPa (FEA). This also applies to angels of around 22.5° and to the results in rolling direction (around 0 degree), see figure 5. The stresses and angles which do not occur for σ_{xx} within the XRD are those with a value between 45° and 90°. This can be caused by the XRD beam diameter of approximately 0.7 mm and thus, the measured values are averaged over the corresponding area. Close to the edges of the specimen, the XRD beam is wider than the sample and thus may cause measurement uncertainties. Additional differences can have an origin in the evolution of the microstructure within the rolled

specimen. Furthermore, the sharp and ideal edges of the specimen within the FEA are an idealization of the reality, which causes a bigger increase of stresses close to the edges.

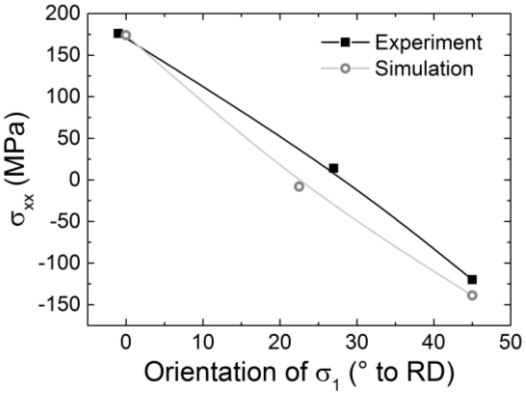

Figure 5. The residual stresses in rolling direction (σ_{xx}) in dependence of the orientation of the 1st principal stress component. The alignment of the points with similar orientations of σ_1 results in a very good agreement between experiment and simulation.

4. Summary and conclusions

Generally, it can be concluded that the principal stresses cannot be analyzed separately. To get an overview of the effective stresses in the specimen, the whole stress tensors given in the results section have to be considered. In this example, the stress state in FEA consists of tensile stresses in the center of the sample and compressive stresses at the edges. This stress characteristic was also measured experimentally. The decay of the tensile stresses as well as the change of the stress orientation from the center of the specimen to the edges numerically occurs at lower distances from the center compared to the experimental values. These differences can be attributed to the idealized sharp edges in the simulation that allow for less deformation compared to the experiment. Generally, the agreement of the residual-stress values is good despite of experimental and numerical uncertainties.

Overall, there are different factors, which have to be considered for cold flat rolling processes, to achieve realistic results within the FEA. Most importantly, no remeshing of the sample should take place within the FEA. During the remeshing process, existing residual stresses can be eliminated and spread over the sample on a new level. In addition to the new distribution of the mesh, the values of the stresses were quite lower than the real stresses or the given stresses of the numerical analysis without remeshing. Hence, the analysis without remeshing shows a much better agreement with the experiment. However, the lack of remeshing causes other problems in further rolling steps such as problematic ratios within the edge lengths of the elements, which possibly reduces the accuracy of the simulation.

Acknowledgement

The authors gratefully acknowledge the Deutsche Forschungsgemeinschaft (DFG) for supporting this work (projects LA 1274/27-1 and AW 6/27-1).

References

[1] Hoffmann H, Neugebauer R and Spur G (Eds.) 2012 *Handbuch Umformen* vol 1 (München: Carl Hanser Verlag)

[2] Kato B and Aoki H 1978 Residual stresses in cold-formed tubes *J. Strain Anal.* **13** 193

[3] Razny W, Fischer F D, Finstermann G, Schwenzfeier W and Zeman K 1996 The influence of some rolling parameters on the residual stresses after rolling *J. Mat. Proc. Technol.* **60** 81

[4] Dixit U S and Dixit P M 1997 A study on residual stresses in rolling *Int. J. Mach. Tools Manufact.* **37** 837

[5] Cruise R B and Gardner L 2008 Residual stress analysis of structural stainless steel sections. *J. Constr. Steel Res.* **64** 352

[6] Moen C D, Igusa T and Schafer B W 2008 Prediction of residual stresses and strains in cold-formed steel members *Thin-Walled Struct.* **46** 1274

[7] Max Baum Stahl Service GmbH, DC04 material data sheet with test results of the used batch.

[8] Eigenmann B and Macherauch E 1996 Röntgenographische Untersuchung von Spannungszuständen in Werkstoffen. Teil III *Matwiss. Werkstofftechn.* **27** 426

[9] Kopp R and Wiegels H (Eds.) 1999 *Einführung in die Umformtechnik* vol 2 (Aachen: Verlag Mainz)

[10] Simufact Engineering GmbH 2015 manual simufact.forming Anwendung